STM JOURNALS

Journal of
Power Electronics & Power Systems

https://journals.stmjournals.com/jopeps

ISSN: 2249-863X (Online)
ISSN: 2321-4244 (Print)
Volume 14, Issue 3, 2024
September–December
DOI (Journal): 10.37591/JoPEPS

Review JoPEPS

Strengthening Low-Voltage Ride-Through in Wind Energy Systems: A Comparative Study of DVR and STATCOM

Bibhu Prasad Ganthia[1,*], Praveen B.M.[2]

Abstract

This study looks at the various methods used to improve the low-voltage ride-through (LVRT) capabilities of wind turbine systems (WT) that are based on double-fed induction generators (DFIG). The Type-III WT machine, which is mostly based on DFIG, is instantly connected to the grid without the digital power interface, making the terminal voltage or reactive electricity output unmanageable. This is because the world utilizes between 20% and 25% of renewable energy from wind. Consequently, new LVRT techniques based on the use of extra-active interface technologies were described in this work. The low-voltage fault problem is now being addressed by a variety of approaches. This research attempts to identify such working ways by bridging the gap in terms of total adaptive performance, operating complexity of controllers, and cost-effectiveness by analyzing LVRT strategies for DFIG-based wind energy conversion system (WECS). Based on their grid integrations, this study focuses on methods to improve LVRT's reliance on relationship establishment in three key areas. The wind turbine system in this study is connected to a dynamic voltage restorer (DVR) and static synchronous compensator (STATCOM) for active and reactive power regulation during the fault detection process. This paper highlights the operation of both synchronous and non-synchronous reference frames. It also shows how the use of STATCOM in conjunction with synchronous reference frame (SRF) theory improves active and reactive power during disturbances. The MATLAB Simulink is used to simulate and analyze the mathematical models of the complete system.

Keywords: DVR, STATCOM, LVRT, DFIG, WT, FACT, WECS

INTRODUCTION

The atmosphere warms because of the intermittent sunshine created by the wind. The pressure levels are the result of the hot and cold air zone formation. Wind flow is caused by air moving from a high-pressure area to a low-pressure area [1–3]. We call the kinetic energy of water "energy in motion." The aerodynamically designed blades of a wind turbine rotate because of this cinematic energy. The blades can never be driven at an electricity-neutral speed by wind alone. The gearbox helps to increase the rotor shaft rpm in some wind energy conversion system (WECS) topologies. The mechanical energy of the shaft is transformed into electrical power by generators. They send this electricity to the grid [4]. A sophisticated device called a WECS transforms wind energy from a kinetic to an electrical form.

The key component of a WECS is a wind turbine, which captures wind through its blades, causing them to rotate as shown in Figure 1. Figure 2 shows a schematic of the network wind power conversion block with both components. Turbine aerodynamic performance is governed by the power coefficient CpC_pCp, which is influenced by the tip speed ratio and blade pitch angle. The rotation of the turbine

*__Author for Correspondence__
Bibhu Prasad Ganthia
E-mail: jb.bibhu@gmail.com

[1]Post Doc Fellow, Department of Electrical and Electronics Engineering, College of Engineering and Technology, Srinivas University, Mangalore, Karnataka, India
[2]Director, College of Engineering and Technology, Srinivas University, Mangalore, Karnataka, India

Received Date: October 11, 2024
Accepted Date: October 28, 2024
Published Date: November 04, 2024

Citation: Bibhu Prasad Ganthia, Praveen B.M. Strengthening Low-Voltage Ride-Through in Wind Energy Systems: A Comparative Study of DVR and STATCOM. Journal of Power Electronics & Power Systems. 2024; 14(3): 47–62p.

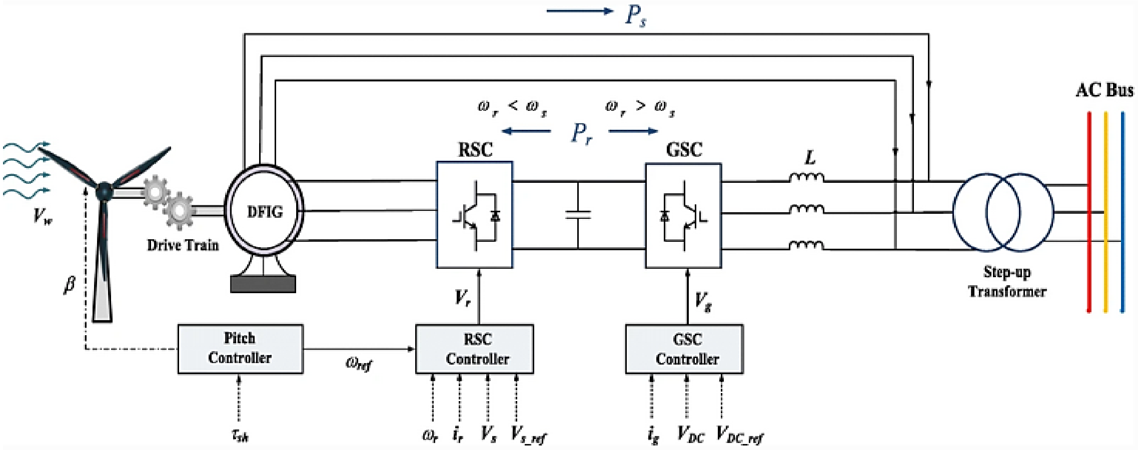

Figure 1. Model of wind energy conversion system.

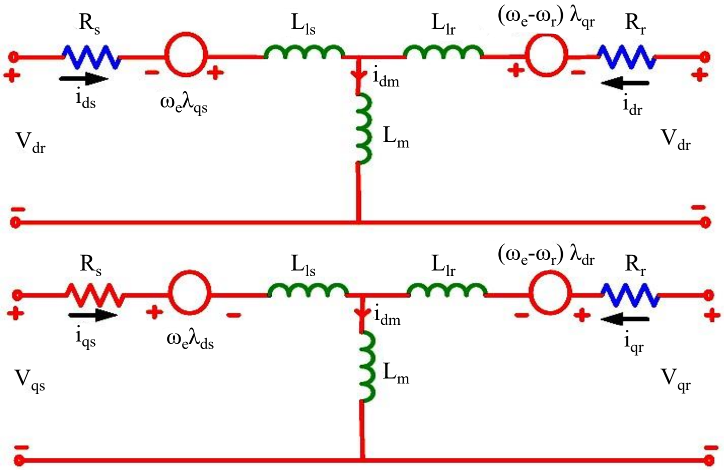

Figure 2. Equivalent circuit diagram of DFIG for both direct axis and quadrature axis.

blades is transferred through a drivetrain, which may include a gearbox to match the low-speed rotation of the turbine with the high-speed requirements of the generator. In some systems, a direct-drive mechanism is used to eliminate the need for a gearbox. The generator, typically a doubly fed induction generator (DFIG), permanent magnet synchronous generator (PMSG), or squirrel-cage induction generator (SCIG), then converts the mechanical energy into electrical energy. Power electronics play a vital role in controlling the output of the WECS, regulating the voltage and frequency, and ensuring grid synchronization, particularly in variable-speed wind conditions. The control system is integral to the WECS, managing various functions, such as turbine blade pitch control, yaw control for wind direction alignment, and generator operation to optimize power output. In grid-connected systems, the control system ensures stability and smooth integration of wind-generated electricity into the grid. Additional components, such as anemometers and wind vanes, provide real-time wind data, whereas transformers adjust the voltage levels for grid compatibility. This WECS model efficiently manages the conversion of wind energy into usable electrical power, thereby contributing to renewable energy generation.

The second type is a wind turbine variable-speed system that uses a double-fed induction generator (DFIG) [5, 6, 8] The DFIG winding stator is directly connected to the grid, and the winding rotor electric converter has a power rate of about 30%. The third type is a variable wind turbo with a SCIG electronic conversion system or fully rated synchronous generator. These two generators usually require a multistage gearbox. Low-ratio gearbox systems (PMSG) can supply direct power to synchronous generators including permanent synchronous magnet generators. An interesting alternative is the use of a single- or two-phase gearbox [7, 9].

DOUBLY-FED INDUCTION GENERATORS

Figure 3 shows the mathematical model of DFIG. It contains every equation in the model, including torque, voltage, and flow equations. In this study, it is assumed that the rotor current is positive to the inflow and the stator current is positive to the outflow. This explains the positive orientation of the current. The diagram below shows the DFIG architecture implemented in a d-q synchronous rotating coordinate system [10].

$$V_{ds} = R_s i_{ds} + d\Psi_{ds}/dt - \omega_{dqs}\Psi_{ds} \quad (1)$$

$$V_{qs} = R_s i_{qs} + d\Psi_{qs}/dt + \omega_{dqs}\Psi_{qs} \quad (2)$$

$$V_{dr} = R_r i_{dr} + d\Psi_{dr}/dt - \omega_{dqr}\Psi_{qr} \quad (3)$$

$$V_{qr} = R_r i_{qr} + d\Psi_{qr}/dt + \omega_{dqr}\Psi_{dr} \quad (4)$$

$$\Psi_{ds} = L_{ss} i_{ds} + L_m i_{dr} \quad (5)$$

$$\Psi_{qs} = L_{ss} i_{qs} + L_m i_{qr} \quad (6)$$

$$\Psi_{dr} = L_m i_{ds} + L_{rr} i_{dr} \quad (7)$$

$$\Psi_{qr} = L_m i_{qs} + L_{rr} i_{qr} \quad (8)$$

$$\text{(Torque) } T_m = 1.5pL_m(i_{qs}i_{dr} - i_{ds}i_{qr}) = 1.5p(\Psi_{ds}i_{qs} - \Psi_{qs}i_{ds}) \quad (9)$$

The voltage, instantaneous current, and flux for each stator winding and rotor winding in the d-q synchronous reference system are denoted by the variables u, i, and ψ in the equations that follow. R_s and R_r represent the stator and rotor resistance of the windings, respectively. The DFIG leakage inductances for the stator and rotor are denoted by Lls and Llr, respectively. L_m Symbolizes the mutual inductance. The stator-side self-inductance is represented by L_{ss}, which satisfies L_{ss}=$L_m + Llr. L_{rr}$. According to the model equation $L_{rr} = L_m$+Llr. ω_{dqs}, L_{rr} stands for the rotor-side self-inductance, while ω_{dqr} represents the stator-side magnetic fields, and ωdqr represents the rotating angular velocity of the rotor-side magnetic field [11, 12].

The equation of the motion of the rotor is defined as follows:

$$T_m - T_e = \frac{J}{P}\frac{dw_r}{dt} \quad (10)$$

where Tm denotes the mechanical torque denoted by T_m. The input torque is applied to the DFIG, Te is the electromagnetic torque of the DFIG, J is the rotational inertia of the DFIG, p is the polar logarithm of the DFIG, and w_r is the DFIG speed [13–15].

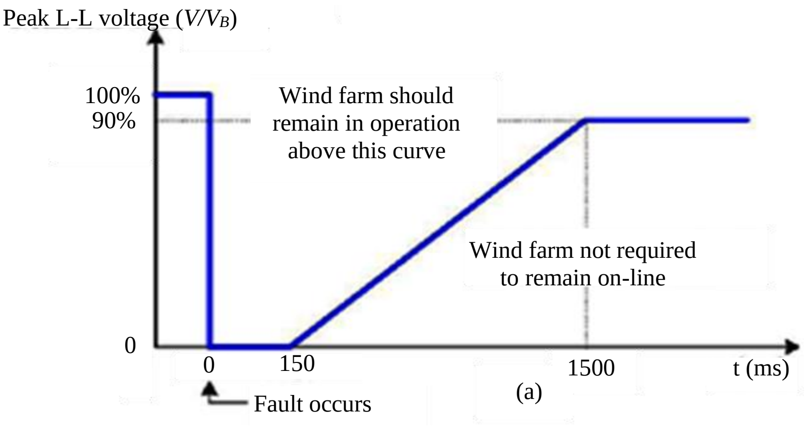

Figure 3. LVRT curve.

LOW-VOLTAGE RIDE-THROUGH TECHNIQUE

Figure 4 shows the rotor-side converter, which supplies power to the rotor windings to activate the induction generator. When compared to PI control with an internal control loop, the actual part of the rotor current irq with irqref is limited to zero. The output of the current controller is the voltage vrq of the rotor-side converter. The necessary 3-phase voltages for the rotor winding are generated by a similarly operated section of the ground and vrd, which drives the ground and irq to their reference values. Stated differently, the rotor-side converter generates varying excitation frequencies based on wind speed [16–20].

One basic approach uses a synchronous dq-axis framework with the d-axis to operate an induction generator based on the position of the stator flux vector. This is referred to as the vector power of the SFO. SFO is the name. It is also possible to provide reactive and active control separately. Typical vector control of inductor generators frequently uses orientation frames, such as rotor-flow orientation and magnetizing flux orientation. The stator-powered direction (SVO) is another frequently used technique in DFIG vector controllers [21–24].

DYNAMIC VOLTAGE RESTORER CONTROL AND OPERATION

Power quality is simply the optimal power supply within voltage and frequency tolerances. The quality of electricity may be due to consumer equipment malfunction. These issues are linked to voltage-related issues that affect the efficiency of electrical equipment, including voltage imbalance, swelling, harmonics, slope, and insufficient power factors.

Energy quality issues include lightning, power outages, equipment failure, and switching disruptions. The user is not sufficiently satisfied, even if the power system employs several filter technologies to obtain the required power quality. To minimize and mitigate instability disadvantages, compensate for them, and increase system dependability, new power electronic controllers have emerged in the past few decades, giving rise to bespoke power. The use of custom power units (CPDs) for effective voltage modification is on the rise, according to the IEEE and IEC standards. Voltage distortions are currently the largest problem for industrial clients among other tension-related problems. CPD is one of the most effective techniques to reduce voltage-related issues. A dynamic voltage restorer (DVR) includes an ICT, a voltage source converter (VSC), an energy-storing unit, and a filter, as illustrated in Figure 4 [25–30].

STATCOM CONTROL AND OPERATION (STATIC SYNCHRONOUS COMPENSATOR)

Static synchronous compensator (STATCOM) is a reactive power-controlled device that can be regulated. By generating or absorbing reactive electricity at the point of a common connection, it provides voltage support without the need for large external or capacitor banks. Figure 5 depicts a basic voltage source conversion system. The converter receives a DC voltage from the charged capacitor Cdc,

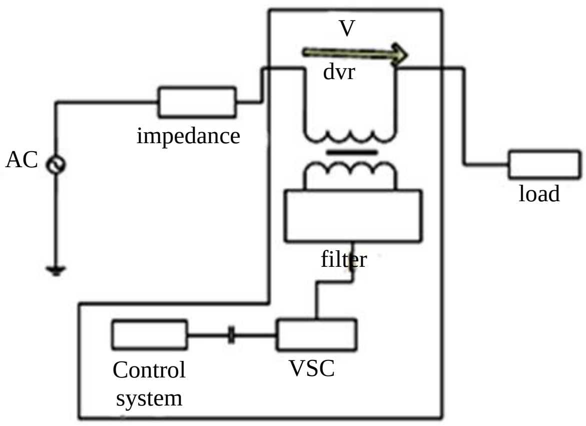

Figure 4. Configuration of dynamic voltage restorer (DVR).

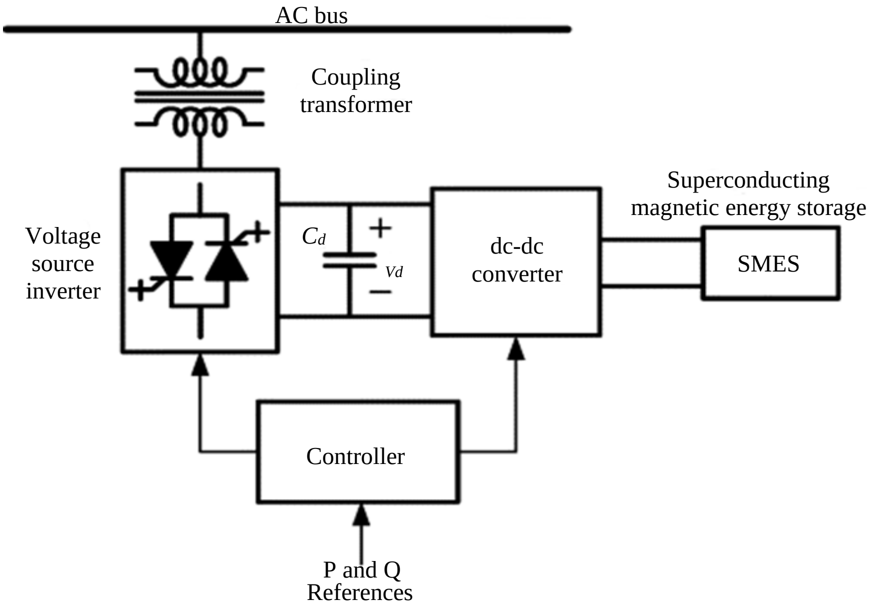

Figure 5. Configuration of static synchronous compensator (STATCOM).

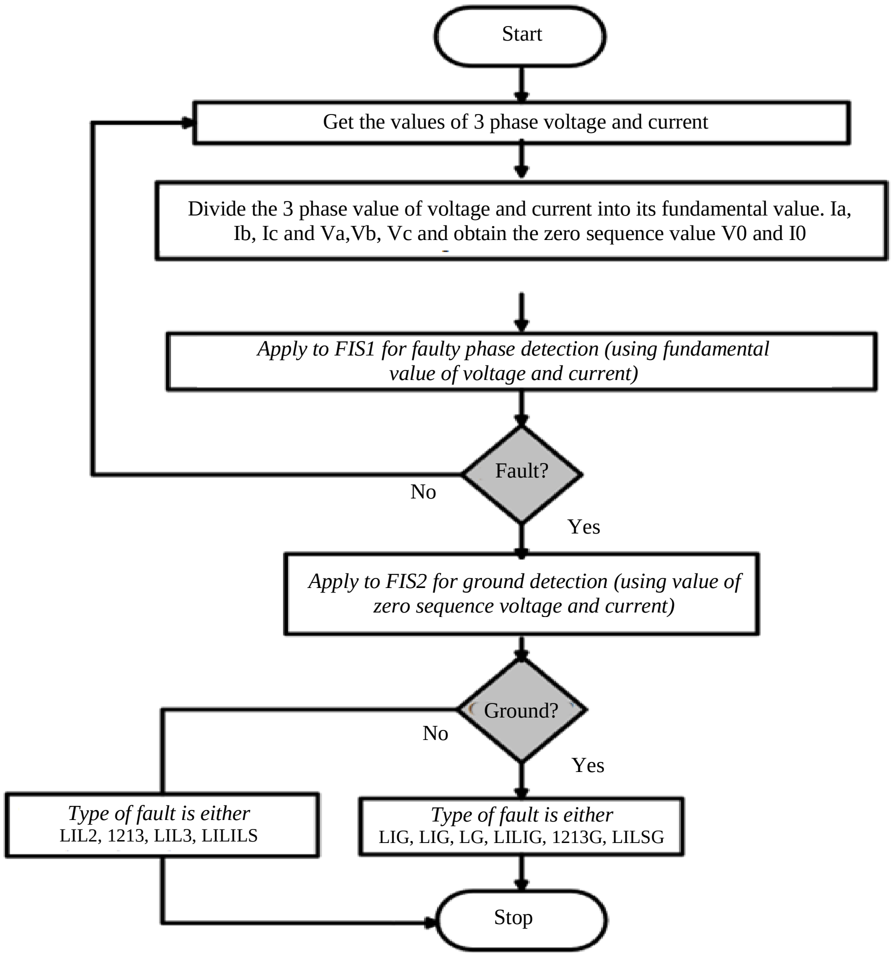

Figure 6. Flow chart for controller fuzzy logic fault current detection.

which generates a set of controlled three-phase output voltages with the AC power system's frequency. By altering the amplitude of the output voltage U, the reactive power exchange of the converter and AC systems can be controlled. When the amplitude of the output voltage U is greater than the AC system's UT, a leading current is produced; in other words, the system recognizes the STATCOM as a conductor and produces reactive power. When the output voltage amplitude decreases below that of an AC system, the STATCOM is considered an inductor, and a trailing current is generated. In this case, the reactive power is absorbed. If the amplitudes were the same, there was no power exchange. There is no such thing as a lossless converter. The phase-angle adjustment method can also be used to control the reactive power generated or absorbed by increasing or decreasing the capacitor voltage UDC and, therefore, the output voltage U as shown in Figure 6. The formula for the transmitted active power is derived from a series of computations.

The characteristics of the STATCOM explicitly demonstrate its ability to manage very low system voltages (as low as 0.15 per unit), which is the value corresponding to the coupling transformer reactance. In contrast to an SVC, which, at the maximum capacitive output, becomes an uncontrolled capacitor bank, this is a stark difference. A STATCOM can maintain the system voltage at very low voltages, as long as the DC capacitor has sufficient energy to supply losses.

Logic Controller with Fuzzy

The flow diagram of the proposed concept is shown in Figure 7. Two related fuzzy inference systems were created. First, to identify the incorrect phase or phases, and second, to identify the ground. The Table 1 shows the guidelines and strategies for their success. The tension and current inputs were used in each step. The FIS file is utilized as a function of triangle membership and is in the Mamdani format. Membership rules are divided into three categories: low, medium, and high. The show is called "trip" and includes triple membership rules. Low flight, edge voyage, and high journey are the three types of line [31–35].

The Notion of Synchronous Reference Frames or SRF Theory

Among the various control systems used in STATCOM, SRF theory is the most reliable and appropriate for DVR and STATCOM. Having a frame rotating at a synchronous velocity is the main idea of this phrase. Table 1 shows the guidelines and strategies for their success. The tension and current inputs were used in each step. The FIS file is utilized as a function of triangle membership and is in the Mamdani format. Membership rules are divided into three categories: low, medium, and high. The show is called "trip" and includes triple membership rules. Low flight, edge voyage, and high journey are the three types of lines [31–35].

The Notion of Synchronous Reference Frames or SRF Theory

Among the various control systems used in STATCOM, SRF theory is the most reliable and appropriate for DVR and STATCOM. Having a frame rotating at a synchronous velocity is the main idea of this phrase. SRF-based controls are of good quality when compared to other methods; however,

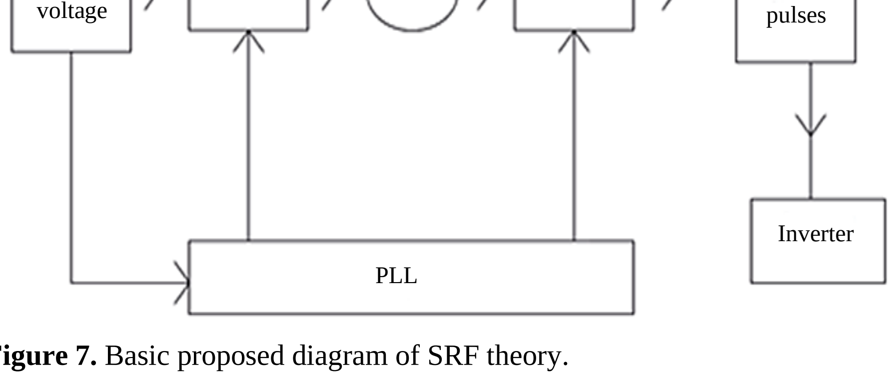

Figure 7. Basic proposed diagram of SRF theory.

they require PLL technology. Based on PLL [36–37], the new phase-locking technique functions under distorted and unbalanced load scenarios. SRF theory is one of the main strategies used in this methodology to lower the THD. The main advantage of the SRF theory is the absence of time-dependent spatial coordinate translation. The Park equation is used in the SRF theory. Through this procedure, three-phase voltages or currents are converted into a synchronously rotating d-q reference frame. By eliminating high-frequency components, the filter system filters the continuous vital components created by the Park's metamorphosis. The DC component of the filter circuit does not produce any phase errors [38–41]. In SRF theory, the three-phase load current is converted to the synchronous d-q referral frame. There is a basic and harmonic component of the d-q currents. Reverse Park transformation was used to create three-phase harmonic signals.

MATLAB SIMULINK DESIGN

As shown in Figure 8, the VSC is a DVR. To address worsening routine voltages and reduce the likelihood of load or generator problems, they are commonly connected to the grid via a line filter (usually an LC type) and serial coupling transformer. Different DVR architectures were evaluated in terms of their power and voltage ratings. Here, the DVR protection system and crowbar protection are compared [42–48]. Good steady-state sinusoidal errors were used to track the positive- and negative-sequence voltage components in each system.

The MATLAB Simulink model for a WECS using a DVR, as shown in Figure 8, integrates a wind turbine, generator, and DVR system to mitigate voltage sags and swells during grid disturbances. A generator (usually a PMSG or doubly fed induction generator) is powered by the mechanical power generated by the wind turbine [49]. Power electronics interfaces ensure a stable voltage and frequency while the generated electrical power is sent to the grid.

The DVR is a key component in this model and is designed to protect the WECS from voltage disturbances in the grid. It operates by injecting the required voltage to maintain the grid voltage levels during faults or fluctuations, thereby effectively stabilizing the system. In the Simulink environment, DVR is modeled using VSCs, energy storage elements (such as batteries or capacitors), and control algorithms [50–54]. The control system continuously monitors the grid voltage, and when a sag or swell is detected, the DVR injects a compensating voltage, ensuring a smooth and uninterrupted operation of the WECS. The Simulink model includes detailed subsystems of the wind turbine, generator, grid connection, and DVR control logic.

The MATLAB Simulink model for a WECS using a STATCOM, as shown in Figure 9, focuses on reactive power compensation and voltage stability in the grid-connected wind energy system. Similar to the previous model, the wind turbine generates electrical power via a generator, which is fed into the electrical grid. However, unlike the DVR model, which directly addresses voltage sags and swells, the STATCOM in this setup enhances grid stability by dynamically managing the reactive power flow. The STATCOM was linked to the grid and WECS at the point of common coupling (PCC) in the Simulink model [55–58]. It is composed of components that may inject or absorb reactive power, such as capacitive or inductive elements, and a VSC. The control system in the STATCOM continuously monitors the grid voltage and adjusts the reactive power accordingly, to maintain the voltage levels within the desired limits. This helps improve power quality, enhances voltage stability, and mitigates issues such as voltage flickers and imbalances caused by fluctuating wind power generation. The Simulink model includes a wind turbine, generator, STATCOM with its control system, and grid interface, offering a comprehensive simulation of the WECS under varying grid conditions.

As shown in Figure 9, the static synchronous compensator is a reactive power-regulated device. To fix the damaged normal voltages and avoid possible load or generator issues, they are typically connected to the grid via a line filter (typically an LC type) and a serial coupling transformer. Various

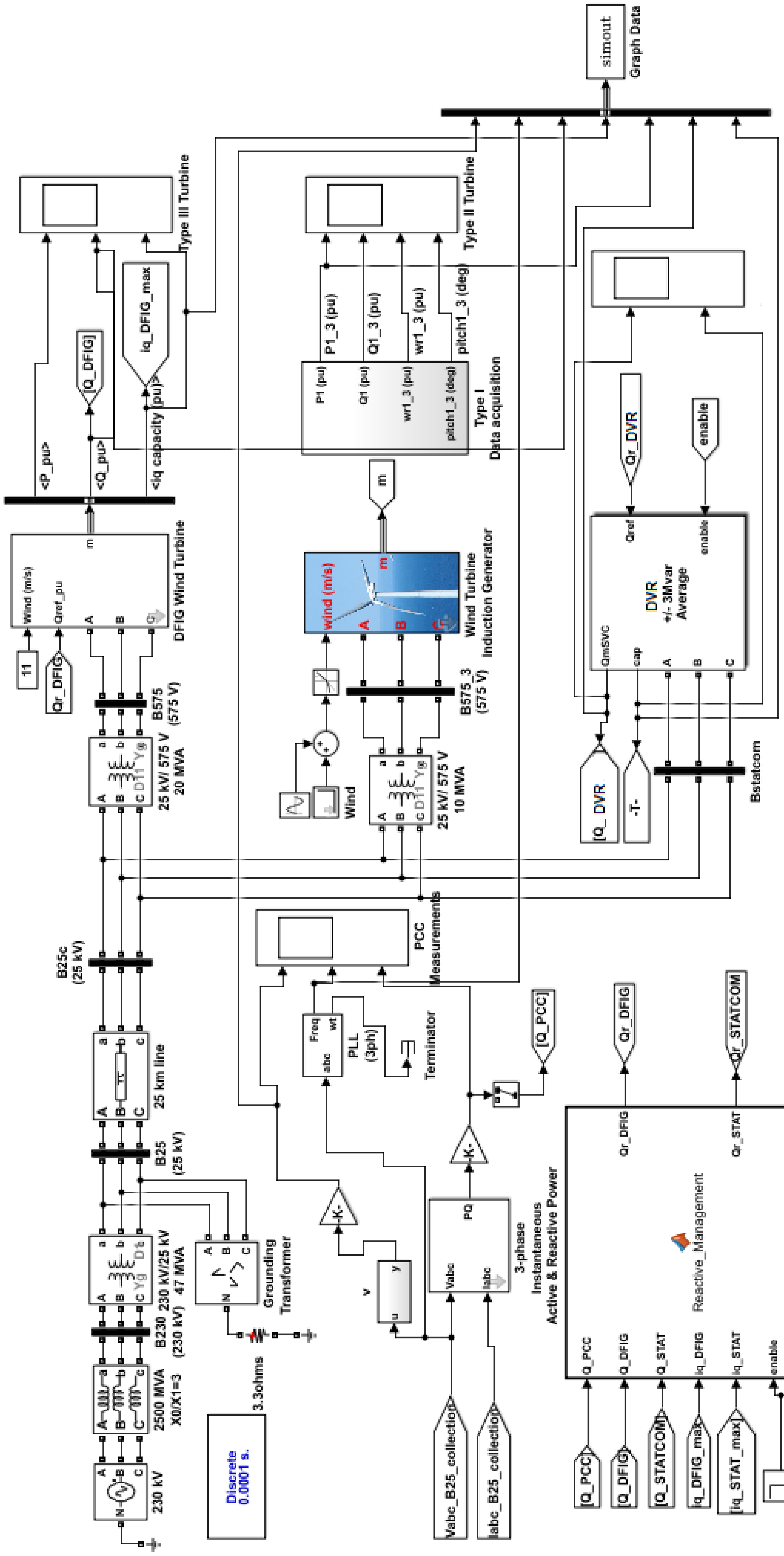

Figure 8. MATLAB Simulink model for WECS using DVR.

Journal of Power Electronics & Power Systems
Volume 14, Issue 3
ISSN: 2249-863X (Online), ISSN: 2321-4244 (Print)

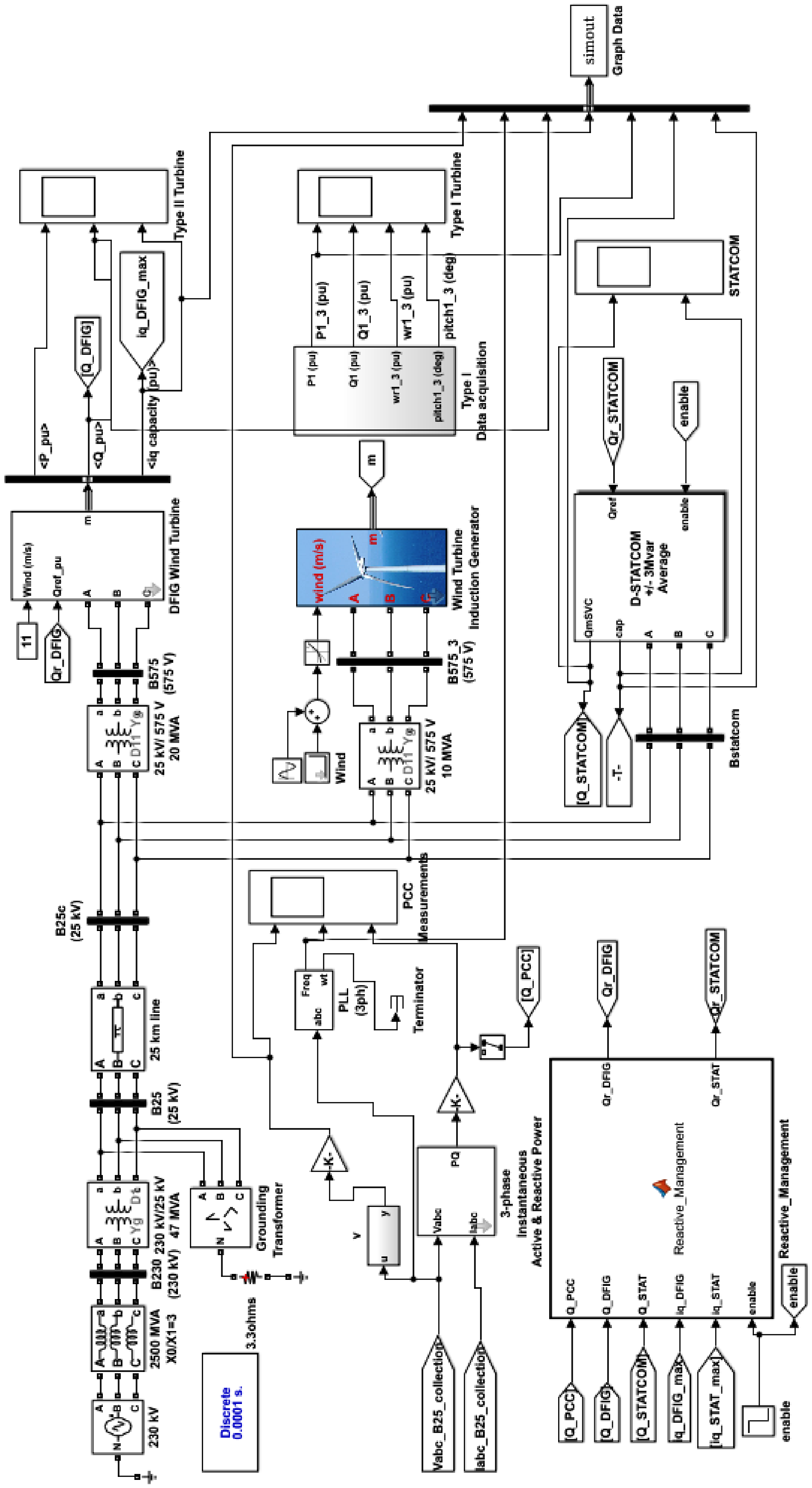

Figure 9. MATLAB Simulink model for WECS using STATCOM.

STATCOM topologies were examined in terms of power and voltage ratings. The crowbar and STATCOM protection systems were compared in this study [59, 60]. Every device tracks positive and negative program voltage constituents with good steady-state sinusoidal errors.

In both MATLAB Simulink, models for WECS using a DVR and STATCOM play critical roles in enhancing the grid stability and power quality. The DVR model was designed to mitigate voltage sags and swells by injecting compensating voltage during disturbances, ensuring continuous and stable WECS operation. On the other hand, the STATCOM model improves voltage stability by dynamically managing reactive power, addressing voltage imbalances, and fluctuations in wind power generation. These models demonstrate effective techniques for integrating the WECS into a grid while maintaining a reliable and stable electrical output.

SIMULINK RESULTS (COMPARISON USING DVR AND STATCOM)

The comparative results using the two Flexible AC Transmission Systems (FACTS devices (DVR and STATCOM) are shown below. Figure 10 illustrates the terminal voltage settling after the transient without SRF theory and Figure 11 illustrates the terminal voltage settling after the transient with SRF theory. MATLAB Simulink findings were used to compare the two FACTS devices: the STATCOM and the DVR. The objective was to analyze how these devices help stabilize the terminal voltage of a WECS under grid disturbances. The comparison is particularly focused on the impact of these devices with and without the use of SRF theory, which is a widely used control strategy for managing grid-connected systems.

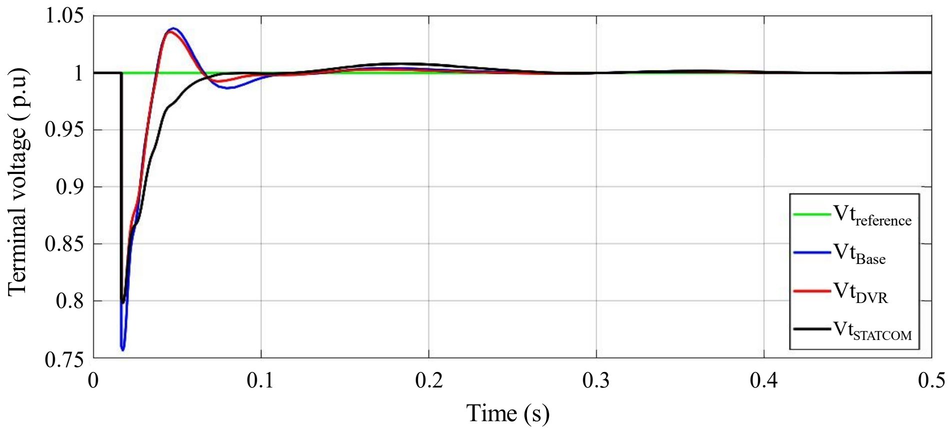

Figure 10. Terminal voltage settling after transient without SRF theory.

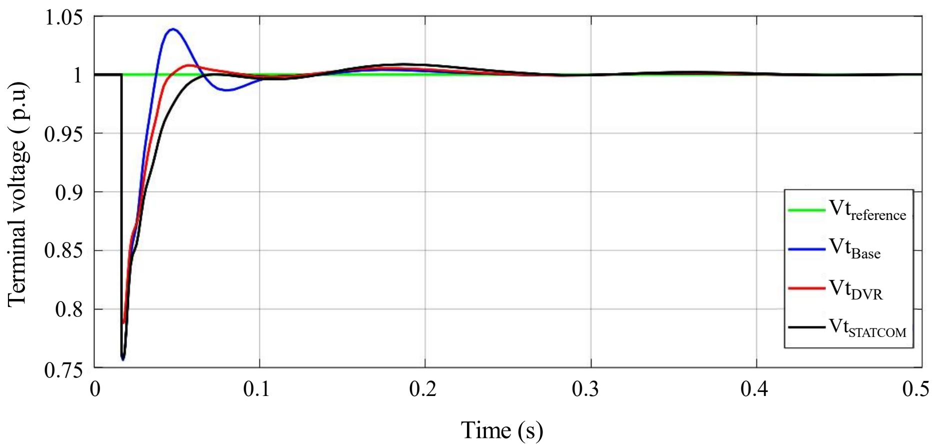

Figure 11. Terminal voltage settling after transient with SRF theory.

In Figure 10, the terminal voltage response of the WECS under grid disturbances *without the use of SRF theory*. Both the DVR and STATCOM are used independently to mitigate voltage fluctuations caused by sudden changes in wind speed or grid faults (such as sags, swells, and other disturbances). Figure 11 illustrates how the terminal voltage behaves after a transient disturbance when no advanced control strategy, such as the SRF Theory, is applied.

DVR Performance

The DVR injects a compensating voltage during transients to restore normal operation. Without the SRF Theory, the DVR responds directly to voltage deviations but may exhibit slower response times and higher settling times because of the lack of precise control in detecting and compensating for unbalanced conditions.

STATCOM Performance

The STATCOM manages reactive power to stabilize the terminal voltage. Without the SRF theory, the STATCOM still provides compensation, but like DVR, it may have a limited dynamic response, resulting in a longer settling time and less efficient voltage regulation under severe transient conditions.

In this scenario, the terminal voltage may exhibit oscillations or a delayed return to steady-state values owing to the absence of advanced control strategies that could enhance the accuracy and speed of the voltage compensation.

In Figure 11, the performance of the DVR and STATCOM is compared with the SRF theory applied as the control mechanism. The SRF theory helps in transforming three-phase voltage signals into a synchronous rotating reference frame, making it easier to detect and control voltage imbalances and disturbances.

DVR Performance with SRF Theory

The DVR response becomes more accurate and faster when SRF theory is applied. DVR can more efficiently detect sags, swells, and other disturbances in real-time and inject a precise compensating voltage. This results in a faster terminal voltage settling with reduced oscillations and improved system stability.

STATCOM Performance with SRF Theory

Similarly, the STATCOM benefits from an SRF control strategy. It can more effectively manage the reactive power and stabilize the terminal voltage more quickly after a disturbance. The SRF theory allows for a more coordinated and dynamic response, improving the overall voltage profile and reducing settling time.

The key differences between the results are shown in Figures 10 and 11 show a *faster voltage settling time and improved stability* when the SRF theory is applied. Without SRF theory, both DVR and STATCOM still perform their roles in compensating for voltage disturbances, but their effectiveness is reduced owing to slower response times and potential overshoot or oscillations in the terminal voltage. With the SRF theory, the control over the grid-tied system is enhanced, allowing for more precise voltage control and reducing the impact of transients on the WECS. Overall, the application of the SRF theory significantly improves the performance of both FACTS devices, with the DVR excelling in voltage compensation during disturbances and the STATCOM effectively managing reactive power to maintain grid stability.

In this study, a comparative analysis of the low-voltage ride-through (LVRT) capability of a WECS using a DVR and STATCOM was thoroughly examined. The objective was to evaluate the effectiveness of these two FACTS devices in stabilizing the terminal voltage under different wind speed variations, with and without the application of the SRF theory. The results indicate that both the DVR and

Table 1. LVRT Capability Settling Times (in milliseconds).

Wind variation (m/s)	Controller	Reference	Base	DVR	STATCOM
4 m/s	Settling time (msec)	11	12	11.3	11.04
8 m/s	Settling time (msec)	12	12.5	12.8	11.2
12 m/s	Settling time (msec)	13	13.5	13.7	12.7
16 m/s	Settling time (msec)	14	14.5	13.9	13.3
Remark	Settling speed		Fast	Faster	Fastest

STATCOM significantly improve the system's ability to handle voltage disturbances during transients. However, the STATCOM demonstrates superior performance in terms of faster settling time and enhanced stability, particularly when the SRF theory is applied. The capability of the STATCOM to dynamically manage reactive power allows it to respond more swiftly to voltage variations, leading to quicker system stabilization. However, the DVR also provides effective voltage compensation, but its performance is slightly slower than that of the STATCOM, particularly at higher wind speed variations. The findings from Table 1 further highlight that both the DVR and STATCOM perform better than the reference controller, with the STATCOM exhibiting the fastest response across all wind variation scenarios. This makes STATCOM a more suitable option for applications requiring rapid voltage stabilization and efficient LVRT capability in a WECS.

In conclusion, while both DVR and STATCOM are effective for enhancing LVRT capability in WECS, STATCOM proves to be a superior solution for applications requiring faster voltage stabilization, making it ideal for more dynamic and variable wind conditions.

CONCLUSION

Voltage modules and angle-independent control are key features that enable STATCOM to produce and consume active and reactive power. A circular power chart was illustrated after the consumed and generated capacities were computed and simulated. From the circular power chart, it can be deduced that the STATCOM generated/consumed power increases in tandem with the converter voltage. Consequently, the amount of electricity generated or consumed increases with the amplitude of the converter voltage. This implies that the converter voltage values can be changed to alter power. Additionally, regulation is accomplished by altering the sinusoidal source phase of the transistor control mechanism.

REFERENCES

1. Siraj K, Siraj H, Nasir M. Modeling and control of a doubly fed induction generator for grid integrated wind turbine. 2014 16th International Power Electronics and Motion Control Conference and Exposition, Antalya, Turkey, 2014. pp. 901–906. DOI: 10.1109/EPEPEMC.2014.6980613.
2. Barick CK, Mohapatra BK, Kabat SR, Jena K, Ganthia BP, Panigrahi CK. Review on scenario of wind power generation and control. 2022 1st IEEE International Conference on Industrial Electronics: Developments & Applications (ICIDeA), Bhubaneswar, India, 2022. pp. 12–17. DOI: 10.1109/ICIDeA53933.2022.9970193.
3. Rubavathy SJ, Venkatasubramanian R, Kumar MM, Ganthia BP, Kumar JS, Hemachandu P, Ramkumar MS. Smart grid based multiagent system in transmission sector. 2021 Third International Conference on Inventive Research in Computing Applications (ICIRCA), Coimbatore, India, 2021. pp. 1–5. DOI: 10.1109/ICIRCA51532.2021.9544644.
4. Zheng W, Mehbodniya A, Neware R, Wawale SG, Ganthia BP, Shabaz M. Modular unmanned aerial vehicle platform design: Multi-objective evolutionary system method. Comput Electr Eng. 2022;99:107838. DOI: 10.1016/j.compeleceng.2022.107838.
5. Rafin SS, Ahmed R, Haque MA, Hossain MK, Haque MA, Mohammed OA. Power electronics revolutionized: A comprehensive analysis of emerging wide and ultrawide bandgap devices. Micromachines. 2023 Oct 31;14(11):2045.

6. Biswal A, Ganthia BP, Satapathy S, Patra S, Bhatta SK, Mohanty M. Prototype design of modified mechanical drive train gear box system using ANSYS for wind power generation. 2nd International Conference on Artificial Intelligence and Smart Energy (ICAIS); Coimbatore, India; 2022. Vol. 2022:518–523. DOI: 10.1109/ICAIS53314.2022.9743077.
7. Priyadarshini L, Kundu S, Maharana MK, Ganthia BP. Controller design for the pitch control of an autonomous underwater vehicle. Eng Technol Appl Sci Res. 2022;12:8967–8971. DOI: 10.48084/etasr.5050.
8. Samal SK, Jena S, Ganthia BP, Kaliappan S, Sudhakar M, Kalyan SS. Sensorless speed control of doubly fed induction machine using reactive power based MRAS. In: Journal of Physics: Conference Series. Vol. 2161, No. 1, p. 012069. IOP Publishing; 2022.
9. Refaai MRA, Dhanesh L, Ganthia BP, Mohanty M, Subbiah R, Anbese EM. Design and implementation of a floating PV model to analyse the power generation. Int J Photoenergy. 2022:1–13. DOI: 10.1155/2022/3891881.
10. Ganthia BP, Barik SK, Nayak B. Sliding mode control and genetic algorithm optimized removal of wind power and torque nonlinearities in mathematical modeled Type-III wind turbine system. 2021 9th International Conference on Cyber and IT Service Management (CITSM), Bengkulu, Indonesia, 2021. pp. 1–7. DOI: 10.1109/CITSM52892.2021.9587933.
11. Ganthia BP, Hanumanthakari S, Gudimindla H, Anandaram H, Ramkumar MS, Mohanty M, Gopal SR, Sarojwal A, Hadish KM. Machine learning strategy to achieve maximum energy harvesting and monitoring method for solar photovoltaic panel applications. Int J Photoenergy. 2022:1–9. DOI: 10.1155/2022/4493116.
12. Maherchandani JK, Joshi RR, Tirole R, Swami RK, Ganthia BP. Performance comparison analysis of energy management strategies for hybrid electric vehicles. In: Recent Advances in Power Electronics and Drives. Springer Nature Singapore; 2022:245–254. DOI: 10.1007/978-981-16-9239-0_18.
13. Kabat SR, Panigrahi CK. Power quality and low voltage ride through capability enhancement in wind energy system using unified power quality conditioner (UPQC). ECS Trans. 2022;107:5655-5662. DOI: 10.1149/10701.5655ecst.
14. Ganthia BP, Choudhury S, Mohanty S, Acharya SK. Mechanical design and power analysis of Type-III wind turbine system using computational fluid dynamics. 2022 IEEE Delhi Section Conference (DELCON), New Delhi, India, 2022. pp. 1–6. DOI: 10.1109/DELCON54057.2022.9753089.
15. Ganthia BP, Barik SK, Nayak B. Radial basis function artificial neural network optimized stability analysis in modified mathematical modeled Type-III wind turbine system using bode plot and Nyquist plot. ECS Trans. 2022;107:5663–5670. DOI: 10.1149/10701.5663ecst.
16. Pahadasingh S, Jena C, Panigrahi CK, Ganthia BP. JAYA algorithm-optimized load frequency control of a four-area interconnected power system tuning using PID controller. Eng Technol Appl Sci Res. 2022;12:8646–8651. DOI: 10.48084/etasr.4891.
17. Ganthia BP, Barik SK, Nayak B, Priyadarshi N, Padmanaban S, Hiran KK, Bansal RC. Power control of modified type III DFIG-based wind turbine system using four-mode type I fuzzy logic controller. Artif Intell Internet Things Renew Energy Syst. 2021;12:41.
18. Mishra S, Ganthia BP, Sridharan A, Rajakumar P, Padmapriya D, Kaliappan S. Optimization of load forecasting in smartgrid using artificial neural network based NFTOOL and NNTOOL. In: Journal of Physics: Conference Series. Vol. 2161, No. 1, p. 012068. IOP Publishing; 2022.
19. Kabat SR, Panigrahi CK, Ganthia BP. Comparative analysis of fuzzy logic and synchronous reference frame controlled LVRT capability enhancement in wind energy system using DVR and STATCOM. In: Sustainable Energy and Technological Advancements. Springer: Singapore; 2022:423–433. DOI: 10.1007/978-981-16-9033-4_32.
20. Ganthia BP, Suriyakrishnaan K, Prakash N, Harinarayanan J, Thangaraj M, Mishra S. Comparative analysis on various types of energy storage devices for wind power generation. In: Journal of Physics: Conference Series. Vol. 2161, No. 1, p. 012066. IOP Publishing; 2022.

21. Ganthia BP, Rana PK, Pattanaik SA, Rout K, Mohanty S. Space vector pulse width modulation fed direct torque control of induction motor drive using MATLAB-simulink. In: 3rd International Conference on Electrical, Electronics, Engineering Trends, Communication, Optimization, and Sciences (EEECOS 2016). IET; 2016. p. 1–5. DOI: 10.1049/cp.2016.1497.
22. Ganthia BP, Barik SK, Nayak B. Genetic Algorithm Optimized and Type-I fuzzy logic controlled power smoothing of mathematical modeled Type-III DFIG based wind turbine system. Mater Today Proc. 2022;56:3355–3365. DOI: 10.1016/j.matpr.2021.10.193.
23. Kabat SR, Panigrahi CK, Ganthia BP, Barik SK, Nayak B. Implementation and analysis of mathematical modeled drive train system in type III wind turbines using computational fluid dynamics. Adv Sci Technol Res J. 2022;16:180–189. DOI: 10.12913/22998624/144753.
24. Sahu PK, Mohanty A, Ganthia BP, Panda AK. A multiphase interleaved boost converter for grid-connected PV system. 2016 International Conference on Microelectronics, Computing and Communications (MicroCom), Durgapur, 2016. pp. 1–6. DOI: 10.1109/Micro Com.2016.7522539.
25. Pritam A, Sahu S, Rout SD, Ganthia S, Ganthia BP. Automatic generation control study in two area reheat thermal power system. IOP Conf Ser: Mater Sci Eng. 2017;225(1):012223. DOI: 10.1088/1757-899X/225/1/012223.
26. Ganthia BP, Mohanty M, Maherchandani JK. Power analysis using various types of wind turbines. In: Modeling and Control of Static Converters for Hybrid Storage Systems. IGI Global; 2022. p. 271–286. DOI: 10.4018/978-1-7998-7447-8.ch010.
27. Ganthia BP, Pritam A, Rout K, Singhsamant S, Nayak J. Study of AGC in two-area hydro-thermal power system. Adv Power Syst Energy Manag. 2016;393–401.
28. Ganthia BP, Abhisikta A, Pradhan D, Pradhan A. A variable structured TCSC controller for power system stability enhancement. Mater Today Proc. 2018;5:665–672.
29. Ganthia BP, Pradhan R, Das S, Ganthia S. Analytical study of MPPT based PV system using fuzzy logic controller. 2017 International Conference on Energy, Communication, Data Analytics and Soft Computing (ICECDS), Chennai, India, 2017. pp. 3266–3269. DOI: 10.1109/ICECDS.2017.8390063.
30. Ganthia BP, Barik SK, Nayak B. Comparative analysis of various types of control techniques for wind energy conversion system. In: Modeling and Control of Static Converters for Hybrid Storage Systems. IGI Global; 2022. p. 143–174. DOI: 10.4018/978-1-7998-7447-8.ch006.
31. Ganthia BP, Barik SK, Nayak B. Wind turbines in energy conversion system: Types & techniques. In: Renewable Energy and Future Power Systems. Springer; 2021. p. 199–217. DOI: 10.1007/978-981-33-6753-1_9.
32. Ganthia BP, Barik SK, Nayak B. Shunt connected FACTS devices for LVRT capability enhancement in WECS. Eng Technol Appl Sci Res. 2020;10:5819–5823. DOI: 10.48084/etasr.3560.
33. Ganthia BP, Agarwal V, Rout K, Pardhe MK. Optimal control study in DFIG based wind energy conversion system using PI & GA. 2017 International Conference on Power and Embedded Drive Control (ICPEDC), Chennai, India, 2017. pp. 343–347. DOI: 10.1109/ICPEDC.2017.8081112.
34. Ganthia BP, Mohanty S, Rana PK, Sahu PK. Compensation of voltage sag using DVR with PI controller. In: International Conference on Electrical, Electronics, and Optimization Techniques (ICEEOT), Chennai, India; 2016. p. 2138–2142. DOI: 10.1109/ICEEOT.2016.7755068.
35. Ganthia B, Mohanty Monalisa, Mohapatra Sushree Shataroopa, Pradhan Rosalin, Satapathy Subhasmita, Patra Shilpa, Pahadasingh Sunita. Artificial Neural Network Optimized Load Forecasting of Smartgrid using MATLAB. Control Syst Optim Lett. 2023;1(1):46–51. Available from: https://www.example.com
36. Ganthia BP, Barik SK, Nayak B. Wind turbines in energy conversion system: Types & techniques. In: Renewable Energy and Future Power Systems. Springer: Singapore; 2021. p. 199–217. DOI: 10.1007/978-981-33-6753-1_9.

37. Ganthia BP, Barik SK, Nayak B. Hardware in loop (THIL 402) validated Type-I fuzzy logic control of Type-III wind turbine system under transients. J Electr Syst. 2021;17:28–51.
38. Ganthia BP, Barik SK. Steady-state and dynamic comparative analysis of PI and fuzzy logic controller in stator voltage oriented controlled DFIG fed wind energy conversion system. J Inst Eng (India): Ser B. 2020;101:273–86. DOI: 10.1007/s40031-020-00455-8.
39. Ganthia BP, Barik SK, Nayak B. Shunt connected FACTS devices for LVRT capability enhancement in WECS. Eng Technol Appl Sci Res. 2020;10:5819–23. DOI: 10.48084/etasr.3560.
40. Ganthia BP, Barik SK, Nayak B. Low voltage ride through capability enhancement using series connected fact devices in wind energy conversion system. J Eng Sci Technol. 2021;16:365–84.
41. Gu J, Wang W, Yin R, Truong CV, Ganthia BP. Complex circuit simulation and nonlinear characteristics analysis of GaN power switching device. Nonlinear Eng. 2021;10:555–62. DOI: 10.1515/nleng-2021-0046.
42. Xie H, Wang Y, Gao Z, Ganthia BP, Truong CV. Research on frequency parameter detection of frequency shifted track circuit based on nonlinear algorithm. Nonlinear Eng. 2021;10:592–9. DOI: 10.1515/nleng-2021-0050.
43. Ganthia BP. Application of hybrid facts devices in DFIG based wind energy system for LVRT capability enhancements. J Mech Cont Math Sci. 2020;15:245–56.
44. Ganthia BP, Barik SK, Nayak B. Transient analysis of grid integrated stator voltage oriented controlled type-III DFIG-driven wind turbine energy system. J Mech Cont Math Sci. 2020;15:139–57.
45. Kabat SR, Ganthia BP, Panigrahi CK. Fuzzy logic and synchronous reference frame controlled LVRT capability enhancement in wind energy system using DVR. Turk J Comput Math Educ (TURCOMAT). 2021;12:4899–907.
46. Joseph L, Ganthia BP. ANN based speed control of brushless DC motor using DC-DC converter. Des Eng. 2021;1998–2011.
47. Ganthia BP, Upadhyaya M. Bridgeless AC/DC converter & DC-DC based power factor correction with reduced total harmonic distortion. Des Eng. 2021;2012–8.
48. Mannam P, Manchireddy S, Ganthia BP. Grid tied PV with reduced THD using NN and PWM techniques. Des Eng. 2021;2019–27.
49. Devraj PA, Subramanian SS, Durairaj U, Ganthia BP, Upadhyaya M. MATLAB/Simulink based THD reduction using active power filters. Des Eng. 2021;1990–7.
50. Durairaj U, Khillo A, Priyadarshini S, Ganthia BP, Koyyeda R. Design and implementation of power system performance improvement by using PFC. Des Eng. 2021;1366–76.
51. Jayakumar N, Devi Vighneshwari B, Mohanty M, Kabat SR, Ganthia BP, Rani NC, et al. Cascade H bridge multilevel inverter with PWM for lower THD, EMI & RFI reduction. Ann Rom Soc Cell Biol. 2021;25(6):2972–7.
52. Thenmalar K, Kiruba K, Raj P, Ganthia BP. A real-time implementation of ANN controller to track maximum PowerPoint in solar photovoltaic system. Ann Rom Soc Cell Biol. 2021;25:10592–607.
53. Ganthia BP, Pradhan R, Sahu R, Pati AK. Artificial ant colony optimized direct torque control of mathematically modeled induction motor drive using PI and sliding mode controller. In: Recent Advances in Power Electronics and Drives. Singapore: Springer; 2021. p. 389–408. DOI: 10.1007/978-981-15-8586-9_35.
54. Pragati A, Ganthia BP, Panigrahi BP. Genetic algorithm optimized direct torque control of mathematically modeled induction motor drive using PI and sliding mode controller. In: Recent Advances in Power Electronics and Drives. Lecture Notes in Electrical Engineering, Vol. 707. Singapore: Springer; 2021. p. 351–66. DOI: 10.1007/978-981-15-8586-9_32.
55. Satpathy SR, Pradhan S, Pradhan R, Sahu R, Biswal AP, Ganthia BP. Direct torque control of mathematically modeled induction motor drive using PI-type-I fuzzy logic controller and sliding mode controller. In: Intelligent Systems. Lecture Notes in Networks and Systems, Vol. 185. Singapore: Springer; 2021. p. 239–51. DOI: 10.1007/978-981-33-6081-5_21.
56. Ganthia BP, Sahu PK, Mohanty A. Minimization of total harmonic distortion using pulse width modulation technique. IOSR J Electr Electron Eng (IOSR-JEEE). 2021; e-ISSN: 2278-1676.

57. Ganthia BP, Rana PK, Patra T, Pradhan R, Sahu R. Design and analysis of gravitational search algorithm based TCSC controller in power system. Mater Today Proc. 2018;5:841–7.
58. Sahu S, Mohapatra BK, Kabat SR, Panda S, Pahadasingh S, Ganthia BP. Multiple order harmonic elimination in photovoltaic system using SPWM based eleven-level cascaded H-BRIDGE multilevel inverter. J Mech Contin Math Sci. 2024;19. DOI: 10.26782/jmcms.2024.08.00002.
59. Ganthia BP, Praveen BM. Review on scenario of wind power generations in India. Electr Eng. 2023;13:1–27.
60. Mohanty M, Nayak N, Ganthia BP, Behera MK. Power smoothening of photovoltaic system using dynamic PSO with ESC under partial shading condition. Proceedings of the 2023 International Conference in Advances in Power, Signal, and Information Technology (APSIT); 2023 Oct 10–12; Bhubaneswar, India. 2023. p. 675–80. DOI: 10.1109/APSIT58554.2023.10201763.

